

### XIII. CONCLUSION

The present paper, like the preceding two,<sup>4,5</sup> emphasizes the need for experimenters to measure and publish additional quantities beyond the positions and widths of resonances; it also emphasizes the possibility that a few parameters may represent observed cross sections more compactly than tables of phase shifts. Although the universal validity of the particular parametrization discussed here is by no means established, the simplicity with which one can determine the parameters from cross-section data and the simple physical interpretation of the parameters suggest that the parametrization merits further attention. I hope these papers will stimulate experimental tests of

formula (1.2) for the description of complicated photoionization cross sections and will encourage publication of profile parameters.

### ACKNOWLEDGMENTS

I am indebted to Dr. David Ederer for questioning the possibility of negative cross sections from Eq. (1.2), to Dr. George Rybicki for discussing biorthogonal expansions, to Dr. Eugene Avrett for explaining radiative transfer equations, and to Professor W. R. S. Garton for inquiring about the CdI, ZnI, and HgI profiles. I have also benefitted from numerous conversations with Dr. David Burgess.

## Optical-Potential Calculation of Electron-Hydrogen Singlet Scattering\*

HUGH P. KELLY

*Department of Physics, University of Virginia, Charlottesville, Virginia*

(Received 11 December 1967)

The use of the optical potential or self-energy of the single-particle Green's function for elastic electron-atom scattering is discussed. The usual formalism, which assumes an unperturbed state described by a single determinant, is generalized to include unperturbed states described by a linear combination of determinants. Calculations are carried out for *S*-wave, elastic, singlet scattering of electrons by hydrogen atoms. The results are compared with the accurate variational calculations by Schwartz.

### I. INTRODUCTION

**P**ERTURBATION expansions for the optical potential for electron-atom scattering have been discussed by many authors<sup>1-7</sup>; and it has been pointed out that the optical potential is the self-energy of the single-particle Green's function.<sup>4-7</sup>

Perturbation calculations have been carried out for electron-atom scattering for helium<sup>8</sup> and for hydrogen.<sup>9</sup> In these calculations the terms in the perturbation expansion were evaluated by methods developed in previous applications of many-body techniques to

bound-state problems.<sup>10-12</sup> In the usual optical-potential or Green's-function formalism, one starts with an unperturbed many-particle state described by a single determinant containing the states of the incident electron and all the atomic electrons. In the case of electron scattering by atoms with closed subshells such as helium, the unperturbed state is described by a single determinant. In the case of electron-hydrogen scattering, the initial unperturbed state of the incident electron and the 1s electron is a single determinant only for the triplet states ( $S=1$ ) with  $M_S=\pm 1$ . Since the phase shift is independent of  $M_S$ , the choice  $M_S=+1$  was made.<sup>9</sup> Calculations for triplet *S*-wave elastic scattering were carried out and compared with the accurate variational calculations of Schwartz.<sup>13</sup> The triplet *S*-wave results of Schwartz are also in close agreement with those of Temkin and Sullivan<sup>14</sup> calculated by solving a set of coupled partial differential equations.

It was found that the second-order optical-potential results, which used Hartree-Fock intermediate states,

\* Work supported in part by the U. S. Atomic Energy Commission and the National Science Foundation Document No. ORO-2915-86.

<sup>1</sup> K. M. Watson, *Phys. Rev.* **89**, 575 (1953).

<sup>2</sup> M. H. Mittleman and K. M. Watson, *Phys. Rev.* **113**, 198 (1959).

<sup>3</sup> B. A. Lippmann, M. H. Mittleman, and K. M. Watson, *Phys. Rev.* **116**, 920 (1959).

<sup>4</sup> J. S. Bell and E. J. Squires, *Phys. Rev. Letters* **3**, 96 (1959).

<sup>5</sup> M. Namiki, *Progr. Theoret. Phys. (Kyoto)* **23**, 629 (1960).

<sup>6</sup> D. J. Thouless, *The Quantum Mechanics of Many-Body Systems* (Academic Press Inc., New York, 1961).

<sup>7</sup> A. L. Fetter and K. M. Watson, in *Advances in Theoretical Physics*, edited by K. A. Brueckner (Academic Press Inc., New York, 1965), Vol. I, p. 115.

<sup>8</sup> R. T. Pu and E. S. Chang, *Phys. Rev.* **151**, 31 (1966).

<sup>9</sup> H. P. Kelly, *Phys. Rev.* **160**, 44 (1967).

<sup>10</sup> H. P. Kelly, *Phys. Rev.* **131**, 684 (1963).

<sup>11</sup> H. P. Kelly, *Phys. Rev.* **136**, B896 (1964).

<sup>12</sup> H. P. Kelly, *Phys. Rev.* **144**, 39 (1966).

<sup>13</sup> C. Schwartz, *Phys. Rev.* **124**, 1468 (1961).

<sup>14</sup> A. Temkin and E. Sullivan, *Phys. Rev.* **129**, 1250 (1963).

gave only approximately 70% of the total correlation contribution to the phase shift. The second-order results are, of course, dependent on the choice of potential used to calculate the intermediate states.<sup>11</sup> The low second-order results in this case are corrected by considering the higher-order diagrams for a single pair of particles. In the scattering problem these are the ladder diagrams and the hole-particle diagrams including exchange. These diagrams are analogous to those for bound-state problems where the second-order energies are too small in magnitude when the Hartree-Fock potential is used.<sup>10</sup> The higher-order diagrams were approximately summed for  $k=0.4$  atomic units (a.u.), and the resulting correlation contribution to the phase shift was found to be 0.0359 as compared with the variational value 0.0365.

In the present work, the optical-potential method is applied to the problem of singlet-state elastic scattering of electrons by hydrogen. Only the  $S$ -wave phase shifts are calculated in this paper. Section II contains a discussion of the modifications in the usual unperturbed single-determinant formalism which must be made in order to carry out the perturbation expansion for an unperturbed state represented by a linear combination of determinants. These considerations apply to any atom in a spherically symmetric ground state ( $L=0$ ). Section III contains numerical results for the singlet  $S$ -wave phase shifts in second order and with estimates of higher-order corrections. Section IV contains a discussion of the results.

## II. PERTURBATION EXPANSION FOR SINGLET STATES

### A. Diagrams

In the singlet-state scattering of electrons by hydrogen (or by any alkali atom), the initial unperturbed state  $\Phi_k$  is a linear combination of determinants

$$\Phi_k = \frac{1}{\sqrt{2}} [(k^+n^-) - (k^-n^+)] \\ = \frac{1}{\sqrt{2}} [\eta_{k^+} \eta_{n^-} - \eta_{k^-} \eta_{n^+}] |0\rangle, \quad (1)$$

where  $(k^+n^-)$  is a determinant containing the incident electron state  $\varphi_k$  with energy  $\frac{1}{2}k^2$  and  $m_s = +\frac{1}{2}$  and also containing the outer bound electron state  $|n\rangle$  with  $m_s = -\frac{1}{2}$  and all single-particle states occupied in the core. The determinant  $(k^-n^+)$  is similar except that the continuum state  $\varphi_k$  has  $m_s = -\frac{1}{2}$  and  $|n\rangle$  is now a state with  $m_s = +\frac{1}{2}$ . The state  $|0\rangle$  contains all the single-particle states of the core. For example, for hydrogen  $|n\rangle = |1s\rangle$  and  $|0\rangle$  is the vacuum. For Li,  $n = 2s$  and  $|0\rangle$  is the core state  $(1s)^2 \uparrow S$ . The operators  $\eta_{k^+}$ ,  $\eta_{n^+}$  are the usual Fermi-Dirac creation operators for states  $|k\rangle$  and  $|n\rangle$ . The state  $\Phi_k$  of Eq. (1) is illustrated in Fig. 1.

The state  $\varphi_k$  is given by

$$\varphi_k(\mathbf{r}) = R(k, l; r) Y_{lm}(\theta, \phi) X_s(m_s), \quad (2)$$

FIG. 1. Linear combination of determinants describing an unperturbed scattering state given by Eq. (1).

$$\frac{1}{\sqrt{2}} \left( \begin{array}{c} \uparrow \\ k^+ \end{array} \begin{array}{c} \uparrow \\ n^- \end{array} - \begin{array}{c} \uparrow \\ k^- \end{array} \begin{array}{c} \uparrow \\ n^+ \end{array} \right)$$

where  $X_s(m_s)$  is a spin eigenfunction, and  $R(k, l; r)$  satisfies the equation (atomic units are used throughout)

$$-\frac{1}{2} [d^2/dr^2 - l(l+1)/r^2] r R(k, l; r) + V_{\text{op}}^{(0)} r R(k, l; r) \\ = \frac{1}{2} k^2 r R(k, l; r). \quad (3)$$

The potential  $V_{\text{op}}^{(0)}$  is a first approximation to the optical potential

$$V_{\text{op}} = V_{\text{op}}^{(0)} + V_{\text{op}}', \quad (4)$$

and

$$R(k, l; r) \rightarrow \sin[kr + (q/k) \ln 2kr - \frac{1}{2}l\pi + \delta_l^{(0)}] / r \quad (5)$$

as  $r \rightarrow \infty$ , where  $V_{\text{op}}^{(0)} \rightarrow q/r$  as  $r \rightarrow \infty$ . If  $V_{\text{op}}$  is used in Eq. (3), we obtain the exact phase shift  $\delta_l$  rather than the approximate  $\delta_l^{(0)}$ .

A good choice for  $V_{\text{op}}^{(0)}$  is

$$V_{\text{op}}^{(0)} = -Z/r + V, \quad (6)$$

where  $V$  is chosen to be the Hartree-Fock potential  $V_{\text{HF}}$ . In the case of triplet scattering from hydrogen,  $V_{\text{HF}}$  is given by

$$V_{\text{HF}}^{tr} \varphi_k(\mathbf{r}) = \int \frac{\varphi_{1s}^*(\mathbf{r}') \varphi_{1s}(\mathbf{r}')}{|\mathbf{r} - \mathbf{r}'|} d\mathbf{r}' \varphi_k(\mathbf{r}) \\ - \int \varphi_{1s}^*(\mathbf{r}') \varphi_k(\mathbf{r}') |\mathbf{r} - \mathbf{r}'|^{-1} d\mathbf{r}' \varphi_{1s}(\mathbf{r}). \quad (7)$$

When  $\Phi_k$  is a single determinant,  $V_{\text{HF}}$  may be defined by its matrix elements

$$\langle a | V_{\text{HF}} | b \rangle = \sum_{n=1}^N (\langle an | v | bn \rangle - \langle an | v | nb \rangle), \quad (8)$$

where the sum includes all  $N$  occupied single-particle states of the atom.

For the case of singlet scattering from hydrogen, the Hartree-Fock equation is<sup>15</sup>

$$\left( -\frac{1}{2} \nabla^2 - \frac{Z}{r} \right) \varphi_k(\mathbf{r}) + \int \frac{\varphi_{1s}^*(\mathbf{r}') \varphi_{1s}(\mathbf{r}')}{|\mathbf{r} - \mathbf{r}'|} d\mathbf{r}' \varphi_k(\mathbf{r}) \\ + \int \frac{\varphi_{1s}^*(\mathbf{r}') \varphi_k(\mathbf{r}')}{|\mathbf{r} - \mathbf{r}'|} d\mathbf{r}' \varphi_{1s}(\mathbf{r}) \\ + (\epsilon_{1s} - \frac{1}{2}k^2) \int \varphi_{1s}^*(\mathbf{r}') \varphi_k(\mathbf{r}') d\mathbf{r}' \varphi_{1s}(\mathbf{r}) = \frac{1}{2}k^2 \varphi_k(\mathbf{r}). \quad (9)$$

In order to correct the Hartree-Fock results we must include the contributions to the phase shift from correla-

<sup>15</sup> B. H. Bransden, A. Dalgarno, T. L. John, and M. J. Seaton, Proc. Phys. Soc. (London) **71**, 877 (1958).

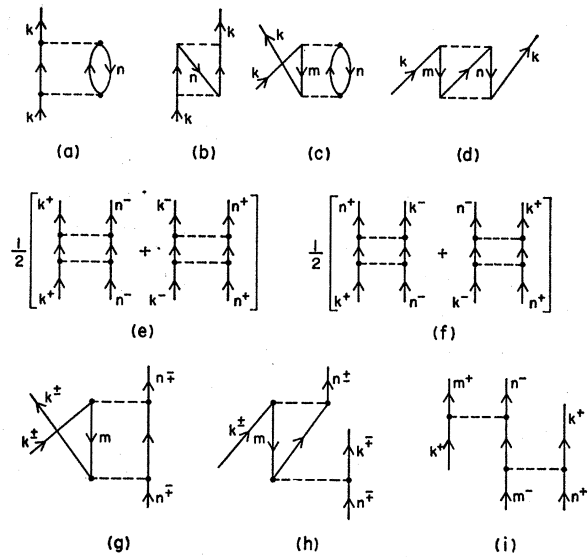


FIG. 2. Second-order diagrams for the optical potential. (a)–(d) Second-order diagrams when  $\Phi_k$  is a single determinant. (e) Diagrams corresponding to (a) when  $\Phi_k$  is given by Eq. (1). (f) Exchange diagrams corresponding to (e). (g) Diagram corresponding to (c). (h) Diagram corresponding to (d). (i) Generalization of (h) when  $m$  is in an open shell.

tions between the incident and atomic electrons. These are accounted for by  $V_{op}'$  which includes the second-order and higher-order terms of the optical potential. Since we now have more than one determinant in  $\Phi_k$ , we must generalize the diagrammatic description<sup>4,6,7</sup> for  $V_{op}$  in the same way as for bound-state problems with more than one determinant included in the unperturbed state  $\Phi_0$ .<sup>12</sup>

In this calculation, the singlet Hartree-Fock equation (9) is used for all physical scattering states. In the diagrams these are the scattering states associated with the free external lines. Since the singlet Hartree-Fock potential is used, the first-order diagrams, including the usual subtracted potential interaction, add to zero. The first-order diagrams in the singlet case include the direct and exchange interaction with  $\varphi_{1s}$  in addition to the subtracted potential interaction. In this case the exchange interaction has a positive sign as in Eq. (9). The direct and exchange interactions in first order are the same as those for second order as shown in Figs. 2(e) and 2(f) except that in first order there is only one Coulomb interaction and no intermediate states.

In Fig. 2, diagrams (a), (b), (c), and (d) are the usual second-order diagrams when  $\Phi_k$  is a single determinant. When  $\Phi_k$  is given by Eq. (1), the diagram of Fig. 2(a) is replaced by the diagrams of Fig. 2(e). The factor of  $\frac{1}{2}$  arises from the  $2^{-1/2}$  which multiplies the determinants of  $\Phi_k$ . If we take the terms of Fig. 2(e) (without the factor  $\frac{1}{2}$ ) and now write out explicitly all the  $\eta^+$  and  $\eta$  operators for each matrix element, we obtain a contribution to  $\hat{V}_{op}'$ , which is the operator corresponding to  $V_{op}$  before integration over the coordinates of the atomic

electrons. We then evaluate  $\langle \Phi_k | \hat{V}_{op}' | \Phi_k \rangle$  with  $\Phi_k$  given by Eq. (1) and we obtain the contribution to  $\langle k | V_{op}' | k \rangle$  given by Fig. 2(e) including the factor  $\frac{1}{2}$ . Similarly, the diagrams of Fig. 2(f) correspond to the exchange diagram of Fig. 2(b). When we calculate  $\langle \Phi_k | \hat{V}_{op}' | \Phi_k \rangle$  with the interactions shown in Fig. 2(f), we obtain the diagrams of Fig. 2(f) with the factor  $\frac{1}{2}$  which is given. We also find that the diagrams of Fig. 2(f) have a positive sign when  $\Phi_k$  is given by Eq. (1), unlike Fig. 2(b) which is always negative.

In the present case the diagram of Fig. 2(c) becomes the diagram given in Fig. 2(g). We actually have two diagrams corresponding to  $(k^+n^-)$  and  $(k^-n^+)$  and each multiplied by  $\frac{1}{2}$  as in Figs. 2(e) and 2(f). For hydrogen, Figs. 2(c), 2(d), 2(g), 2(h), and 2(i) do not exist since there is only one atomic electron. Figure 2(h) is a generalization of Fig. 2(d). In Figs. 2(g) and 2(h) it is assumed that the state  $\varphi_m$  is common to both determinants; that is,  $\varphi_m$  included in the core state  $|0\rangle$  of Eq. (1) and so we may draw hole lines referring to  $\varphi_m$  in the usual way.<sup>4,16,17</sup> In the most general case,  $\varphi_m$  and  $\varphi_n$  both are in an open shell and there are diagrams like Fig. 2(i) multiplied by the appropriate squares of Clebsch-Gordan coefficients which describe the linear combination of determinants in  $\Phi_k$ . In the states  $\varphi_n$  and  $\varphi_m$  are both occupied in  $|0\rangle$ , the diagrams of Figs. 2(a)–2(d) may be used.

In this paper the optical potential is applied to the singlet-state elastic scattering of  $S$ -wave electrons from hydrogen. Since the Hartree-Fock potential is used, the only second-order diagrams are those of Figs. 2(e) and 2(f). Both terms of Fig. 2(e) are equal, and the factor of 2 is cancelled. The expression for Fig. 2(e) is

$$\sum_{k', k''} \frac{\langle kn | v | k'k'' \rangle \langle k'k'' | v | kn \rangle}{(\frac{1}{2}k^2 + \epsilon_n - \epsilon_{k'} - \epsilon_{k''})}, \quad (10)$$

where the sums include only excited single-particle states. The expression for Fig. 2(f) is obtained by replacing the left matrix element by  $\langle nk | v | k'k'' \rangle$  in Eq. (10).

Third-order diagrams for a single electron pair are shown in Fig. 3. These interactions occur in all higher orders and modify all the second-order diagrams of Figs. 2(e) and 2(f). Figure 3(a) is a ladder diagram. In Figs. 3(b) and 3(c) are shown the interactions of excited states with the potential used to calculate them. There are also corresponding diagrams for the interactions of particles with all the occupied unexcited states. For the case where  $\Phi_k$  is a single determinant, the net interaction of particles with the potential and with the passive unexcited states leads to hole-particle diagrams.<sup>9</sup>

In calculating diagrams, we require a complete set of single-particle states which includes the unexcited

<sup>16</sup> J. Goldstone, Proc. Roy. Soc. (London) **A239**, 267 (1957).

<sup>17</sup> H. P. Kelly, Phys. Rev. **166**, 47 (1968).

states  $|n\rangle$ . For hydrogen, the familiar states calculated with only the Coulomb field of the nucleus satisfy this criterion. However, the Hartree-Fock triplet states also have this property.<sup>9</sup> In this case, the set consists of  $|1s\rangle$  and excited states, all of which are triplet scattering states in the Hartree-Fock approximation. It is amusing to note that these triplet states may be used as intermediate states in the singlet (or other) scattering calculations. The fact that the excited particles do not propagate in the triplet potential is corrected by the diagrams like Figs. 3(b) and 3(c) and by interactions with the passive unexcited states. The interactions of Fig. 3 are repeated in fourth-order and higher-order diagrams. The Hartree-Fock triplet states from a previous electron-hydrogen triplet scattering calculation<sup>9</sup> are used in the present calculation. The third-order and higher-order diagrams of Fig. 3 are approximately included.

### B. Phase Shifts

The exact phase shifts  $\delta_l$  may be related to the Hartree-Fock phase shifts  $\delta_l^{(0)}$  and to  $V_{op}'$  by the following expression<sup>9</sup>:

$$\exp(i\delta_l) \sin \delta_l = \exp(i\delta_l^{(0)}) \sin \delta_l^{(0)} - (2m/\hbar^2 k) \exp(i\delta_l + i\delta_l^{(0)}) \langle \varphi_{k,l} | V_{op}' | \psi_{k,l} \rangle. \quad (11)$$

The states  $\varphi_{k,l}$  and  $\psi_{k,l}$  are defined by Eq. (2), and by Eq. (3) with the potentials  $V_{op}^{(0)}$  and  $V_{op}$ , respectively. The normalization of  $\varphi_{k,l}$  and  $\psi_{k,l}$  is given by Eq. (5). We define

$$\Delta\delta_l = \delta_l - \delta_l^{(0)}. \quad (12)$$

When  $V_{op}'$  is small relative to  $V_{op}^{(0)}$ , we may expand in  $(\delta_l - \delta_l^{(0)})$  and approximate  $\psi_{k,l}$  by  $\varphi_{k,l}$ . The result is

$$\Delta\delta_l \approx - (2m/\hbar^2 k) \langle \varphi_{k,l} | V_{op}' | \varphi_{k,l} \rangle, \quad (13)$$

which was first derived<sup>8</sup> from a variational expression for  $\delta_l$ .

Equation (13) has been used to calculate  $\Delta\delta_l$  for electron-helium scattering<sup>8</sup> and for electron-hydrogen scattering in the triplet state.<sup>9</sup> In these cases,  $\Delta\delta_l$  was found to be fairly small and therefore not inconsistent with the approximations leading to Eq. (13). However, in the case of singlet elastic scattering of electrons from hydrogen, the  $\Delta\delta_l$  are found to be larger, and it is desirable to use the exact expression given by Eq. (11). We now wish to have a good knowledge of  $|\psi_{k,l}\rangle$  or at least a reasonable estimate of  $|\psi_{k,l}\rangle - |\varphi_{k,l}\rangle$ . If we knew  $V_{op}'$  rather than just the single matrix element  $\langle k | V_{op}' | k \rangle$ , we could obtain  $\psi_{k,l}$  by solving Eq. (3) with  $V_{op}^{(0)}$  replaced by  $V_{op}^{(0)} + V_{op}'$ .

A rough estimate of  $V_{op}'$  may be obtained<sup>18</sup> by approximating  $V_{op}'$  with

$$\mathcal{U}_p(r) = -\alpha_d/2(r^2 + s^2)^2, \quad (14)$$

<sup>18</sup> M. L. Goldberger and K. M. Watson, *Collision Theory* (John Wiley & Sons, Inc., New York, 1964), p. 853.

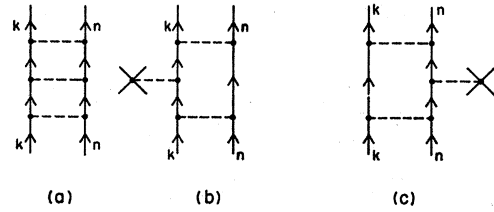


FIG. 3. Third-order diagrams for the optical potential for a given pair of electrons ( $kn$ ). (a) Ladder diagram. (b) and (c) are particle interactions with the potential  $V$ . There are also corresponding interactions with all occupied unexcited states.

where  $\alpha_d$  is the dipole polarizability and  $s$  is a length related to the atomic size. Mittleman and Watson<sup>2</sup> estimate

$$s^4 \approx \frac{1}{2} \alpha_d Z^{1/3}. \quad (15)$$

If the correct phase shift  $\delta_l$  is known, then we might use  $\alpha_d$  in Eq. (14) as an adjustable parameter to obtain  $\delta_l$  from the solution of Eq. (3) with  $V_{op}^{(0)}$  replaced by  $V_{op}^{(0)} + \mathcal{U}_p(r)$ . This would give an approximate  $\psi_{k,l}$  which we denote by  $\psi_{k,l}^{(ap)}$ . For simplicity, we use a fixed value of  $s$  from Eq. (15) calculated with the known dipole polarizability. Since in general we do not know  $\delta_l$  exactly, we can calculate  $\langle \varphi_{k,l} | V_{op}' | \varphi_{k,l} \rangle$  and then obtain a first estimate of  $\delta_l$  from Eq. (13). We then calculate  $\psi_{k,l}^{(ap)}$  with  $\mathcal{U}_p(r)$  by varying  $\alpha_d$  of Eq. (14) until the resulting solution has the phase shift  $\delta_l$ . We evaluate  $\langle \varphi_{k,l} | V_{op}' | \psi_{k,l}^{(ap)} \rangle$  and then substitute into Eq. (11) to solve for a more exact  $\delta_l$ . If necessary, we solve again for  $\psi_{k,l}^{(ap)}$  with the improved value for  $\delta_l$  and repeat the procedure. We may also approximate the solution of  $\delta_l$  by extrapolation. When we have calculated  $\langle \varphi_{k,l} | V_{op}' | \psi_{k,l}^{(ap)} \rangle$  for a given  $\delta_l^{(a)}$ , we may expand Eq. (11) in powers of  $(\delta_l - \delta_l^{(0)})$  and also make the approximation (assuming  $\delta_l^{(a)}$  is close to  $\delta_l$ )

$$\begin{aligned} & \langle \varphi_{k,l} | V_{op}' | \psi_{k,l}^{(ap)} \rangle - \langle \varphi_{k,l} | V_{op}' | \varphi_{k,l} \rangle \\ & \approx ((\delta_l - \delta_l^{(0)}) / (\delta_l^{(a)} - \delta_l^{(0)})) \\ & \times [\langle \varphi_{k,l} | V_{op}' | \psi_{k,l}^{(ap)} \rangle_{\delta_l = \delta_l^{(a)}} - \langle \varphi_{k,l} | V_{op}' | \varphi_{k,l} \rangle]. \end{aligned} \quad (16)$$

We then obtain an approximate solution of Eq. (11). This entire approach, of course, can only give an estimate of the errors incurred in using Eq. (13) rather than the exact expression of Eq. (11).

In principle, we might calculate

$$V_{op}' = \sum_{k,k'} |k\rangle \langle k | V_{op}' | k' \rangle \langle k' |, \quad (17)$$

where the sums over  $k, k'$  now include the complete set of single-particle states. Given  $V_{op}'$ , we could then solve exactly for  $\delta_l$ . However, each matrix element requires a considerable calculational effort, and there is an advantage in expressions such as Eqs. (11) or (13) which only require a single matrix element of  $V_{op}'$ , although we may calculate several matrix elements in approximating  $\langle \varphi_{k,l} | V_{op}' | \psi_{k,l} \rangle$ .

TABLE I. *S*-wave phase shifts (in radians) for electron-hydrogen scattering in the singlet state.

$k$ (a.u.)	$\delta_{\text{HF}}^a$	$\delta_{\text{var}}^b$	$\delta_{\text{var}} - \delta_{\text{HF}}$
0.10	2.39577	2.553(1)	0.157(3)
0.20	1.87012	2.0673(9)	0.1972(7)
0.30	1.50807	1.6964(5)	0.1883(8)
0.40	1.23948	1.4146(4)	0.1751(6)
0.50	1.03147	1.202(1)	0.170(6)
0.60	0.86904	1.041(1)	0.172(1)
0.70	0.74413	0.930(1)	0.186(0)
0.80	0.65126	0.886(1)	0.234(8)

<sup>a</sup> Hartree-Fock phase shifts calculated with Eq. (9).

<sup>b</sup> Phase shifts calculated by Schwartz using the variational principle. See Ref. 13. Figures in parentheses indicate the uncertainty in the last digit.

### III. NUMERICAL RESULTS

Electron-hydrogen *S*-wave, singlet phase shifts were calculated in the Hartree-Fock approximation by solving Eq. (9). The results are given in Table I and are compared with the accurate variational phase shifts of Schwartz.<sup>13</sup> The present Hartree-Fock phase shifts are in good agreement with those calculated previously by John.<sup>19</sup> It is seen from Table I that the differences between the variational and Hartree-Fock results are rather large. This indicates large contributions to phase shifts from the correlations between the incident electron and the 1s electron of hydrogen. In the singlet case the correlation contributions to  $V_{\text{op}}$  are given by the diagrams of Figs. 2(e) and 2(f), by the interactions of Fig. 3, and by the interactions of Fig. 3 in higher orders.

The second-order diagrams of Figs. 2(e) and 2(f) were calculated with intermediate excited Hartree-Fock states used in a previous electron-hydrogen scattering calculation.<sup>9</sup> All the intermediate states are in the

TABLE II. Singlet phase-shift corrections (in radians) due to second-order terms of the optical potential.<sup>a</sup>

	$\Delta\delta_0(l=0)^b$	$\Delta\delta_0(l=0)^b$	$\Delta\delta_0(l=2)^b$	$\Delta\delta_0^c$	$(\delta_{\text{var}} - \delta_0^{(0)})^d$
	$k=0.20$ a.u.				
Direct	0.01151	0.08754	0.01423	0.21586	0.1972(7)
Exchange	0.01062	0.07837	0.01359		
	$k=0.40$ a.u.				
Direct	0.01201	0.06724	0.01061	0.17042	0.1751(6)
Exchange	0.01146	0.05905	0.01005		
	$k=0.60$ a.u.				
Direct	0.01520	0.05756	0.00873	0.15109	0.172(1)
Exchange	0.01493	0.04681	0.00786		
	$k=0.80$ a.u.				
Direct	0.02261	0.05486	0.00824	0.15606	0.234(8)
Exchange	0.02245	0.04091	0.00699		

<sup>a</sup> Calculated by Eq. (13).

<sup>b</sup> The  $l$  values in parentheses refer to the  $l$  values of the intermediate states  $k'$  and  $k''$  used for  $\langle k | V_{\text{op}} | k \rangle$  as given by Eq. (10).

<sup>c</sup> Sum of the second-order direct and exchange terms with  $l=0, 1$ , and 2 intermediate states.

<sup>d</sup> The exact value for  $\Delta\delta_0$  based on the accurate variational calculations of Schwartz listed in Table I. Figures in parentheses indicate uncertainty in the last digit. The values for  $\delta_0^{(0)}$  are the Hartree-Fock singlet results and are listed as  $\delta_{\text{HF}}$  in Table I.

continuum,<sup>9</sup> and the sums are carried out by numerical double integrations as described previously.<sup>9,10</sup> In Figs. 2(e) and 2(f) the states labeled  $k$  were calculated by Eq. (9), the singlet Hartree-Fock equation. The state  $|n\rangle$  is the 1s state of hydrogen. The contributions of these diagrams to the phase shifts were obtained from Eq. (13) and are summarized in Table II.

The second-order values are too high for low  $k$  and become too small at  $k=0.80$ . We note that the inelastic threshold for electron-hydrogen scattering occurs at  $k=0.866$ . In the previous triplet calculation<sup>9</sup> it was found that the second-order results give only approximately 70% of the exact values; this discrepancy was removed by including the higher-order interactions of the types shown in Fig. 3. For atoms larger than hydrogen, there are also interactions with passive unexcited states corresponding to the interactions with the potential shown in Figs. 3(b) and 3(c). The net effect of these interactions gives the hole-particle diagrams in the case where  $\Phi_k$  is a single determinant.<sup>9</sup> The third-order terms of Fig. 3 and these interactions to all higher orders were evaluated by approximations used in previous calculations.<sup>9,10</sup> For example, the ratio of the third-order ladder diagram of Fig. 3(a) to the corresponding second-order diagram is denoted by  $t$ . It has been found that to a good approximation  $t$  is equal to

$$t(k''', k''') = \left[ \left( \frac{2}{\pi} \right)^2 \int_0^\infty dk' \int_0^\infty dk'' \langle k'' k'' k'' | v | k' k'' \rangle \right. \\ \left. \times D(k', k'')^{-1} \langle k' k'' | v | kn \rangle \right] / \langle k'' k'' k'' | v | kn \rangle, \quad (18)$$

where

$$D(k', k'') = \frac{1}{2}k^2 + \epsilon_n - \frac{1}{2}k'^2 - \frac{1}{2}k''^2. \quad (19)$$

The values of  $k''', k''''$  are chosen to be typical excitations of importance in the second-order calculations. Usually  $t(k''', k''''')$  is insensitive to the exact choice of  $k''', k''''$ . The state  $k''''$  is chosen to have the same  $l$  value as  $k'$  and  $k''''$  has the same  $l$  value as  $k''$ . There are also  $l$ -changing ladder diagrams in which the  $l$  value of  $k''''$  differs from that of  $k'$ . The ratio of the diagram of Fig. 3(b) (plus interactions with passive unexcited states) to the second-order diagram is written as  $a_b + b_b$ , where  $a_b$  comes from the part of  $V_{\text{HF}}$  with a direct interaction with  $|n\rangle$  and  $b_b$  comes from the exchange interaction with  $|n\rangle$ . Both interactions are included in  $V_{\text{HF}}$ , and  $V$  in this calculation is  $V_{\text{HF}}$ . The ratio of the diagram of Fig. 3(c) to the corresponding second-order diagram is written  $a_c + b_c$ . The total of the third-order contributions for electron-hydrogen scattering or for correlations only between  $|k\rangle$  and  $|n\rangle$  for any atom is given by  $l$ -changing ladder diagrams, plus the second-order result for  $\langle \varphi_{k,l} | V_{\text{op}} | \varphi_{k,l} \rangle$  (denoted  $\langle \varphi_{k,l} | V_{\text{op}} | \varphi_{k,l} \rangle^{(2)}$ ) times the factor  $(t + a_b + b_b + a_c + b_c)$ . Except for  $l$ -changing ladder diagrams, the ratio of fourth-order to third-order diagrams for the pair  $(kn)$  is given by the same factor, and we may sum this

<sup>19</sup> T. L. John, Proc. Phys. Soc. (London) **76**, 532 (1960).

geometric series to obtain

$$\begin{aligned} \langle \varphi_{k,l} | V_{op}' | \varphi_{k,l} \rangle \\ = \langle \varphi_{k,l} | V_{op}' | \varphi_{k,l} \rangle^{(2)} (1-t-a_b-b_b-a_c-b_c)^{-1} \\ + l\text{-changing ladder diagrams.} \quad (20) \end{aligned}$$

We may also use Eq. (20) with  $\langle \varphi_{k,l} | V_{op}' | \varphi_{k,l} \rangle$  and  $\langle \varphi_{k,l} | V_{op}' | \varphi_{k,l} \rangle^{(2)}$  replaced by  $\langle \varphi_{k,l} | V_{op}' | \psi_{k,l} \rangle$  and  $\langle \varphi_{k,l} | V_{op}' | \psi_{k,l} \rangle^{(2)}$ , respectively. Values for the constants of Eq. (20) are listed in Table III for  $k=0.40$  and  $l=1$ . The value for  $t$  was obtained by the approximation of Eq. (18) with  $k'''=k''''=1.0$ . The constants  $a_b$ ,  $b_b$ ,  $a_c$ , and  $b_c$  were obtained by the same type of approximation, and this approximation is discussed in more detail in Ref. 9. The  $l$ -changing ladder diagrams were estimated as 10% of

$$\langle \varphi_{k,l} | V_{op}' | \varphi_{k,l} \rangle^{(2)} \times (1-t-a_b-b_b-a_c-b_c)^{-1}.$$

Values for  $t$ ,  $a_b$ ,  $b_b$ ,  $a_c$ , and  $b_c$  were found to be similar for  $k=0.2$ ,  $0.4$ , and  $0.6$ . They were approximately 15% larger for  $k=0.80$ . Estimates for the  $l$ -changing diagrams were based on a calculation of these terms for Be correlation energies.<sup>10</sup> We note that the sum of these diagrams is negative relative to  $\langle \varphi_k | V_{op}' | \varphi_k \rangle$  and reduces the magnitude of  $\langle \varphi_k | V_{op}' | \varphi_k \rangle$ . It would, of course, be more accurate to calculate these terms explicitly, and it is hoped that this will be done in a future investigation.

Estimates of contributions from higher-order diagrams and from  $\langle \varphi_{k,l} | V_{op}' | (\psi_{k,l} - \varphi_{k,l}) \rangle$  are listed in Table IV. The estimates of  $\langle \varphi_{k,l} | V_{op}' | (\psi_{k,l} - \varphi_{k,l}) \rangle$  were first obtained by the method discussed at the end of the previous section in which an approximate  $\psi_{k,l}$  is obtained with  $\mathcal{U}_p(r)$  approximating  $V_{op}'$ . In using Eqs. (14) and (15) the fixed value  $s=1.22$  obtained from the hydrogenic value 4.50 for  $\alpha_d$  was used; and  $\alpha_d$  in Eq. (14) was varied to give the correct  $\delta_l$ . For example,  $\alpha_d$  in Eq. (14) was found to be 1.63 for  $k=0.40$  and 1.90 for  $k=0.80$ . The approximation for  $V_{op}'$  given by Eq. (14) is expected to be valid, however, only for the non-exchange diagrams since exchange contributions to  $V_{op}'$  are not proportional to  $r^{-4}$  as  $r \rightarrow \infty$ . From Table II it is seen that the exchange terms contribute approximately one-half of  $\langle \varphi_{k,l} | V_{op}' | \varphi_{k,l} \rangle^{(2)}$ .

In order to obtain a rough approximation to  $\langle \psi_{k,l} - \varphi_{k,l} \rangle$  from the exchange terms, the Hartree-Fock singlet equation [Eq. (9)] was solved with a constant  $A_0$  added to  $(\epsilon_{1s} - \frac{1}{2}k^2)$  which multiplies  $\int \varphi_{1s}^*(r') \varphi_k(r') dr' \varphi_{1s}(r)$  in the last term on the left side of Eq. (9). The resulting effective potential is then closer in form to what is expected for  $V_{op}'$  from exchange contributions than is  $\mathcal{U}_x(r)$  given by Eq. (14). With this exchange approximation for  $V_{op}'$ , the method of the previous section was used to estimate  $\langle \psi_{k,l} - \varphi_{k,l} \rangle$  by varying  $A_0$  until the correct  $\delta_l$  was obtained. Since exchange terms contribute approximately one-half of  $\langle \varphi_{k,l} | V_{op}' | \varphi_{k,l} \rangle$ , the final estimate for  $-(2/k)\langle \varphi_{k,l} | V_{op}' | (\psi_{k,l} - \varphi_{k,l}) \rangle$  of Table IV was obtained by taking an average of the

TABLE III. Ratios of third-order diagrams to second-order diagrams for  $k=0.40$  a.u. and intermediate states with  $l=1$ .<sup>a</sup>

$t$	-0.3131
$a_b$	0.3299
$b_b$	-0.0539
$a_c$	0.3458
$b_c$	-0.0609

<sup>a</sup> Calculated with the approximation of Eq. (18).

results obtained with  $A_0$  and with  $\mathcal{U}_p(r)$  given by Eq. (14). For  $k=0.80$ , the result listed is that obtained by using only the approximation of Eq. (14). When the average is taken as for the other  $k$  values, the result is approximately zero and  $\Delta\delta_l(\text{calc})$  becomes 0.200.

#### IV. DISCUSSION

In the previous sections it has been shown how the optical-potential or Green's-function approach may be applied to the singlet scattering of electrons by hydrogen or by alkali atoms. This extension may be applied to any atom with spherical symmetry, so that the phase-shift analysis is valid. In this more general case,  $\Phi_k$  is given by a linear combination of determinants as in Eq. (1) with the coefficients given by the appropriate Clebsch-Gordan coefficients. Diagrams as listed in Figs. 2(e) and 2(f) are then weighted by the products of Clebsch-Gordan coefficients.

In this paper the  $S$ -wave, singlet scattering of electrons by hydrogen has been calculated below the inelastic threshold. As shown in Table I, there are large differences between the Hartree-Fock results and the accurate variational results of Schwartz.<sup>13</sup> We note that in the singlet scattering the exchange contributions add to the direct terms, unlike the triplet case. The second-order calculated corrections listed in Table I are in fairly good agreement with the differences between the "exact" phase shifts  $\delta_l$  and the Hartree-Fock phase shifts  $\delta_l^{(0)}$  except for  $k=0.80$ . In the triplet case,<sup>9</sup> all the second-order results calculated with Hartree-Fock intermediate states were too low. This indicates in the present calculation that for  $k=0.20$ ,  $0.40$ , and  $0.60$  there may be substantial cancellation between the higher-order diagrams of Fig. 3 and the correction term

TABLE IV. Corrections to the second-order calculations for  $\Delta\delta_0$  (in radians).<sup>a</sup>

$k$ (a.u.)	Higher-order terms <sup>b</sup>	$-(2/k)\langle \varphi_{k,l}   V_{op}'   (\psi_{k,l} - \varphi_{k,l}) \rangle^c$	$\Delta\delta_0$ (calc) <sup>d</sup>	$\Delta\delta_0$ (exact)
0.20	1.199	-0.0595	0.2006	0.1972 (7)
0.40	1.197	-0.0167	0.1884	0.1751 (6)
0.60	1.212	-0.00543	0.1786	0.172 (1)
0.80	1.276	0.00919	0.2098	0.234 (8)

<sup>a</sup> Second-order results are given in Table II.

<sup>b</sup>  $\langle \varphi_{k,l} | V_{op}' | \varphi_{k,l} \rangle / \langle \varphi_{k,l} | V_{op}' | \varphi_{k,l} \rangle^{(2)}$  calculated by Eq. (20). The estimated contributions from  $l$ -changing ladder diagrams are included.

<sup>c</sup> Estimated by methods described in Sec. II.

<sup>d</sup> Calculated by Eq. (11).  $\Delta\delta_0 = \sin^{-1} [-(2/k)\langle \varphi | V_{op}' | \psi \rangle]$ . The term  $-(2/k)\langle \varphi | V_{op}' | \psi \rangle$  is obtained for a given  $k$  by multiplying the second-order result for  $\Delta\delta_0$  in Table II by the number listed under "higher-order terms" in this table and then adding to it  $-(2/k)\langle \varphi | V_{op}' | \psi - \varphi \rangle$  listed above.

$-(2/k)\langle\varphi_{k,l}|V_{op}'|\psi_{k,l}-\varphi_{k,l}\rangle$  because of the use of Eq. (13) in calculating second-order results. This is verified in Table IV where these effects have been estimated. The estimates listed under "higher-order terms" are believed to be accurate to within 5% except for  $k=0.80$ . It is not surprising that there is more uncertainty at  $k=0.80$  since the inelastic threshold occurs at  $k=0.866$ . The constant part of the energy denominator of Eq. (18) is quite small at  $k=0.80$  and the approximation of Eq. (18) is less accurate than it is for larger values of  $\frac{1}{2}k^2+\epsilon_n$ . For example,  $\frac{1}{2}k^2+\epsilon_n=-0.18$  at  $k=0.80$  and  $-0.320$  at  $k=0.60$ . Near the inelastic threshold we might expect better results to be obtained with use of a set of excited states corresponding to single-particle excitations which could describe inelastic processes, unlike the present excited states, all of which are in the continuum. That is, we could use hydrogenic states including  $2s$ ,  $2p$ , etc., and continuum states. This set of states could also describe resonances below the inelastic threshold.<sup>17</sup>

The estimates of  $\langle\varphi_{k,l}|V_{op}'|\psi_{k,l}-\varphi_{k,l}\rangle$  based on the method of Sec. II are somewhat uncertain, and it would be desirable to obtain more information concerning the functional form of  $V_{op}'$ .

The separate contributions to  $\delta_i$  from excited states with  $l=0$  and  $l=1$  in Table II and including higher-order effects compare satisfactorily with the corresponding values listed by Schwartz.<sup>20</sup>

<sup>17</sup> C. Schwartz, Phys. Rev. **126**, 1015 (1962).

One further consideration is the omission of excited states with  $l\geq 3$ . A detailed discussion of the convergence in  $l$  for second-order energies and for phase shifts has been given by Schwartz.<sup>20</sup> In the present calculations the contributions from second-order terms with  $l\geq 3$  are estimated to be small but not completely negligible. However, it is estimated that the second-order terms with  $l\geq 3$  will be reduced significantly by the third-order  $l$ -changing ladder diagrams containing one pair of intermediate states with  $l\geq 3$  and another pair with  $l=0, 1$ , or  $2$ .

*Note added in proof.* These calculations did not include the effect of the nonorthogonality of the scattering solutions to the  $1s$  state beyond the Hartree-Fock term in Eq. (9). Inclusion of this correction might account for the discrepancy for  $k=0.80$  in Table IV.

The numerical results obtained in this calculation indicate the feasibility of applying this optical potential approach to other atoms, and calculations are planned for many  $S$ -state atoms.

#### ACKNOWLEDGMENTS

I am grateful to the late Professor M. E. Rose for his support and encouragement. I also wish to acknowledge helpful discussions with Professor R. A. Ferrell and with Dr. M. Rho, Dr. A. Ron, Dr. H. Schmidt, and Dr. F. Schwabel. I am also grateful to Professor A. Batson and his staff at the Computer Science Center of the University of Virginia for help with the calculations.

## Hyperfine Structure in the Millimeter Spectrum of Hydrogen Sulfide: Electric Resonance Spectroscopy on Asymmetric-Top Molecules

R. E. CUPP, R. A. KEMPF, AND J. J. GALLAGHER

*Martin Marietta Corporation, Orlando, Florida*

(Received 14 July 1967; revised manuscript received 21 February 1968)

The magnetic hyperfine structure of the  $1_{-1} \leftrightarrow 1_1$  rotational transition of  $H_2S$  has been fully resolved in a millimeter electric-resonance spectrometer. The hyperfine components have been measured with an accuracy of 2 parts in  $10^{10}$ . The hyperfine coupling constants are determined to be

$$\begin{aligned} C_{ss} &= 16\,726 \pm 30 \text{ Hz (spin-spin),} \\ C_{1_{10}} &= -16\,239 \pm 10 \text{ Hz (spin-rotation constant for } 1_1 \text{ rotational state),} \\ C_{1_{01}} &= -15\,885 \pm 10 \text{ Hz (spin-rotation constant for } 1_{-1} \text{ rotational state).} \end{aligned}$$

The center frequency of the rotational transition is determined to be  $\nu_0 = 168, 762, 762, 373 \pm 20$  Hz. Several sources of frequency shift and line distortion have been investigated. Seven rotational transitions of hydrogen sulfide have been observed, four of them in the electric-resonance spectrometer. The electric-resonance technique has been extended to a wavelength of  $813 \mu$  by observation of the  $4_0 \leftrightarrow 4_2$  rotational transition of  $H_2S$ .

#### INTRODUCTION

THE first electric-resonance experiment in the millimeter-wavelength region was performed<sup>1</sup> in 1963 on the diatomic molecule  $Li^6F^{19}$ . This investiga-

tion, performed on a collaborative basis, raised several interesting questions which could not be answered during the short time allowed for the experiment. Thus, it was left unanswered whether sufficient spectral purity of the originating source was available to observe Ramsey patterns<sup>2</sup> in the millimeter region, and, if such

<sup>1</sup> L. Wharton, W. Klemperer, L. P. Gold, R. Strauch, J. J. Gallagher, and V. E. Derr, J. Chem. Phys. **38**, 1203 (1963).

<sup>2</sup> N. F. Ramsey, Phys. Rev. **76**, 996 (1949).